

METHOD OF EXTRACTING SWITCHING LOSS FROM A HIGH EFFICIENCY MOSFET BASED HALF BRIDGE CONVERTER.

David Finn, Geoff Walker and Paul Sernia.

School of Information Technology and Electrical Engineering
The University of Queensland, St Lucia, QLD 4072 Australia
Email: dfinn@itee.uq.edu.au

Abstract

The measurement of losses in high efficiency / high power converters is difficult. Measuring the losses directly from the difference between the input and output power results in large errors. Calorimetric methods are usually used to bypass this issue but introduce different problems, such as, long measurement times, limited power loss measurement range and/or large set up cost.

In this paper the total losses of a converter are measured directly and switching losses are exacted. The measurements can be taken with only three multimeters and a current probe and a standard bench power supply. After acquiring two or three power loss versus output current sweeps, a series of curve fitting processes are applied and the switching losses extracted.

1. INTRODUCTION

Measuring the power loss of a high efficiency converter is not an easy task. In high efficiency converters, the error resulting from a direct measurement of power loss (difference between input and output powers) is unacceptable. For this reason losses in high efficiency converters are either measured directly, needing a high-speed oscilloscope and specialised test circuitry, or calorimetric, needing expensive test equipment and/or long period of time.

If losses in high efficiency converters could be measured directly, it would be extremely useful. It has been noted that with any power electronic converter there is only a weak dependence on the output voltage. The form of the loss equations dictate that the power loss is almost entirely dependent on output current. The relationship between power loss and output voltage is only indirectly related through input and output ripple currents. The input ripple current causes loss in the bus capacitors and the output ripple current causes an additional RMS loss in the circuit resistances.

If the output voltage is set to zero volts (shorted), then the power loss of the converter is simply the input power. Due to the extremely low output voltage the duty cycle is always kept low, hence the input capacitance ESR loss and increased resistance loss due to the output current RMS component is also kept very low.

As a case study, this paper will characterise the switching losses in the Tritium Gold 20kW solar car controller. This controller demonstrates the concept well, due to its high efficiency. This switching loss would be hard to find with other methods [1,3,4].

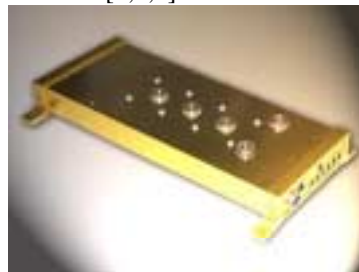


Figure 1 - Tritium Gold Controller

2. CONVERTER LOSSES

The reason for setting the output voltage to zero is simply to allow the converters' loss to be measure directly at the accuracy of the measurement device. If the converter is operating at say 95% efficiency rather than almost 0% efficiency with zero output voltage, then even with measurements accurate to 0.5% there is still a 20% error in the loss measurement. This is quite easy to show with the following equation

$$1.005P_m - 0.995 * .95P_m / 0.05P_m = 1.195 \quad (1)$$

Note that this error gets worst as converter efficiency continues to increase.

To be able to meaningfully present this method of extracting switching losses and justify it, an understanding of the converter losses and their relationship to the output current is required.

In a MOSFET based controller the power loss is related to the output current in the form of $ax^2 + bx + c\sqrt{x} + d$ (2). A list of which components effect what terms in equation (2) and how is given below.

Coefficient of:

(i) *Squared*

Any resistive part of the circuit will have a squared relationship. The resistances are chosen to give the appropriate power loss using average output current instead of device RMS current. The RMS currents were calculated use equations from appendix 1 of [6].

- Low side FET R_M
- High side FET DR_M
- Part of the Commutation Diode. This is the slope of the diode V-I curve after the initial turn on forward drop. $(1-D)R_D$
- Input Capacitors DR_C
- Output inductance R_L

(ii) *Linear*

- Part of the Commutation Diode. $(1-D)V_f$
- Part of the switching loss. $\frac{1}{2}(t_{on} + t_{off})V_{in}f_s$ [5]. t_{on} may also include the reverse recovery time, which is proportional to $\sqrt[4]{I_{out}}$ [1] and therefore also mostly constant.

(ii) *Square Root*

- Reverse recovery charge. The reverse recovery charge has to come directly from the bus and is for the most part proportional to $\sqrt{I_{out}}$ [1].

(iv) *Constant*

- FET Output Capacitance switching loss. Charge and discharge of the FET output capacitance every switching cycle.
- Low voltage system power draw.

In an IGBT converter all the switches have a linear conduction loss component as well as the tail current loss[8], which is also linear. The reverse recovery loss is still present but causes a lot less due to the separate and optimised commutation diodes.

In this method, equation (2) and sections of are used to perform fits to data and extract coefficient and hence switching losses.

3. EXPERIMENTAL RIG

As mentioned in the introduction a Tritium Gold controller was used as the device under test (D.U.T.). Figure 2 shows the layout of the experiment.

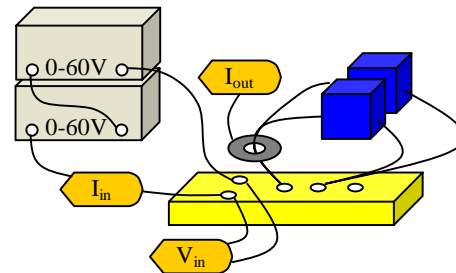


Figure 2 - Experimental Setup.

Known component values:

(i) *Inductors*

Two paralleled CSIRO wheel motor inductors. Four E65 cores per inductor of 3C90 ferrite.

- 7.5mR resistance in parallel
- <0.2W core loss at max ripple of 3A [9,10]

(ii) *MOSFETs*

Three paralleled FETs per switch. IXYS MOSFETs; the IXFX120N20s.

- Resistance of 17mR each, 3|| = 5.6mR [7].
- Turn on voltage drop of 0.6V and an internal resistance of 1mR [7].

4. EXPERIMENTAL PROCEDURE & RESULTS

The PWM of the converter was used as the control for output current. This ensured steady state current. The PWM was stepped in intervals that gave relatively even current steps. Sweeps of power loss versus output current were performed at four different switching frequencies: 20k, 15k, 10k and 5kHz. These are shown in Figure 3 as the x's on curves (a), (b), (c) and (d) respectively.

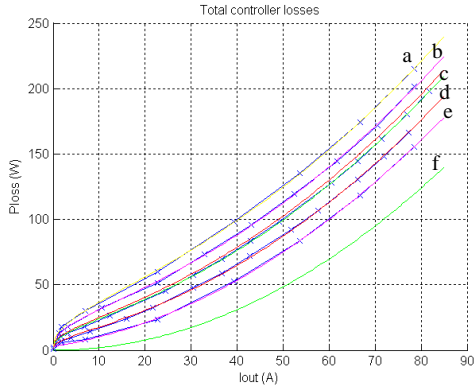


Figure 3- Total Power Loss vs Output current.

The first assumption that is made is that the I^2R component of the losses is constant at all switching frequencies. The low side MOSFET and the output inductors dominate the circuit resistance. There are also the high side MOSFET (DR_M), the commutation diode ($(1-D)R_D$) and the input capacitance ESR (DR_C). These three resistances are only small, and are also obviously dependent on duty cycle but not switching frequency.

All the acquired data points are merged and equation (2) is fitted. This fitted curve can be seen just above curve (c) of Figure 3 and the four different components of this equation are shown in Figure 4. The ax^2 part of equation (2) is extracted and plotted as curve (f) of Figure 3. This is the I^2R term to be used for all the different switching frequencies.

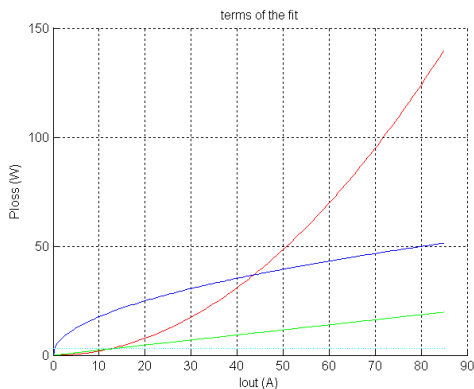


Figure 4 - Components of composite fit

The next assumption that must be made is that the duty cycle is the same between different switching frequencies with the same output current. Given that the duty cycle can be shown to be dependent on only the output current, this seems like a reasonable assumption.

$$D = \frac{(R_M + R_L)I_o + R_D I_o + V_f}{V_{in} - (R_M + R_C)I_o + R_D I_o + V_f}$$

is the duty cycle for a given I_o . This takes into account all five

resistances and the forward drop of the commutation diode. Note there is no relationship to switching frequency; this was also noted experimentally.

A constant duty cycle across all switching frequencies of the same output current means that the input capacitance ESR loss ($DI_o^2 R_C$) is also constant across all switching frequencies of the same output current.

The I^2R component of the power loss is now removed from the original data and the best possible fits are made to the non-resistive losses. These non-resistive loss curves, which are shown in Figure 5, are generated simply by subtracting curve (f) of Figure 3 from the original data points.

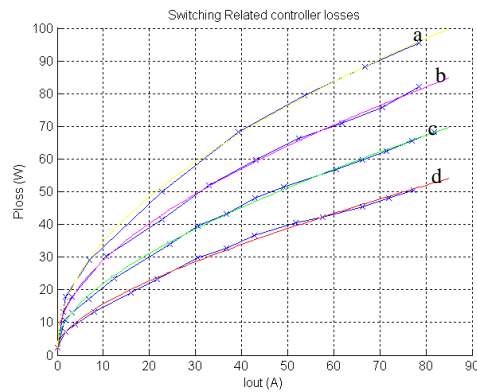


Figure 5 - Non-resistive power losses

Figure 5 shows the non-resistive power loss data points of the four different switching frequencies 20k, 15k, 10k and 5k, (a), (b), (c), and (d) respectively. The next step is to fit curves of the form $bx + c\sqrt{x} + d$ (3) to these data points, these fits are shown in Figure 5 as the coloured curves.

As a check to see if using the same I^2R term in all the curves is accurate, the fitted non-resistive power loss curves are added to the I^2R term found from the original data. These are the coloured curves that lie on the original data of Figure 3. These curves fit almost perfectly, reinforcing the theory that the equivalent resistance does not change between switching frequencies.

It is important to note that non-resistive power losses are not completely composed of switching losses. There is still the linear loss from the 0.6V forward drop of the IXFX120N20 MOSFETs in the D.U.T. The constant power usage of the low voltage system is also still included.

The surest way to remove all other losses and only leave switching losses is to look at the differences between power losses of different switching frequency rather than their absolute

values. The switching losses are linear with switching frequency. Therefore, the difference between the curves of Figure 5 relates to a switching loss. This switching loss is the loss at the frequency equal to the difference in the original frequencies. Table 1 shows the six difference options from Figure 5.

Curve		Curve		Equiv Freq	x Factor
a	-	b	=	5kHz	4
a	-	c	=	10kHz	2
a	-	d	=	15kHz	4/3
b	-	c	=	5kHz	4
b	-	d	=	10kHz	2
c	-	d	=	5kHz	4/3

Table 1 - Switching loss creation table.

The multiplication factors of table 1 are used to scale the fitted equivalent switching frequency losses back to 20kHz.

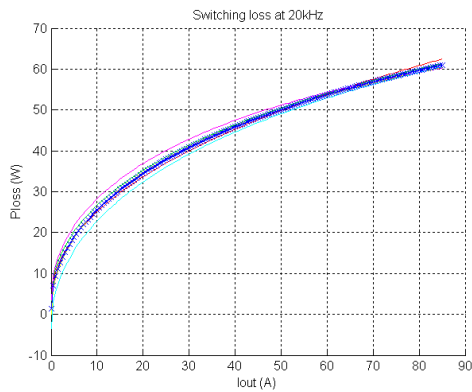


Figure 6 - Switching losses versus output current at 20kHz & Vin = 120V.

The six different curves of Table 1 are all plotted on the graph of Figure 6. As well as the original six curves a seventh final switching loss curve is calculated and shown, this is the thick curve. This curve is simply the least squares fit of all the others. At worst case all of these curves are within $\pm 10\%$ of the final switching loss curve.

As a check of the method's validity the final switching loss curve is subtracted from the original data to create non-switching loss data. Curves of the form $ax^2 + bx + d$ are fitted to these non-switching loss data and the coefficients of these curves were recorded. The coefficients are shown in Table 2.

Input Voltage	Switching Frequency	Equivalent Resistance	Forward Voltage Drop	Low Voltage Power Consumption
40	5k	17.3m	0.5945	2.9333
40	10k	17.3m	0.5951	3.0267
40	15k	17.1m	0.6057	2.9642
40	20k	17.3m	0.5961	2.9976
80	5k	16.5m	0.6275	2.6043
80	10k	16.9m	0.6037	2.7096
80	15k	16.8m	0.6089	2.7441
80	20k	17.3m	0.5742	3.0217
120	5k	16.9m	0.6104	2.5654
120	10k	17.7m	0.5547	3.0150
120	15k	17.9m	0.5308	3.7488
120	20k	17.7m	0.5569	2.8528
Average Values		17.225m	0.5882	2.9320
Average Deviation		0.2962m	0.02096	0.1821

Table 2 - Non-Switching loss coefficients

The focus thus far has been on the 120V case, as it is closer to the normal operating voltage of the D.U.T. Data for input voltages of 40V and 80V were also acquired, as is obvious from Table 2. The switching losses for these input voltages were extracted in the same way and are shown in Figure 7 (40V) and Figure 8 (80V).

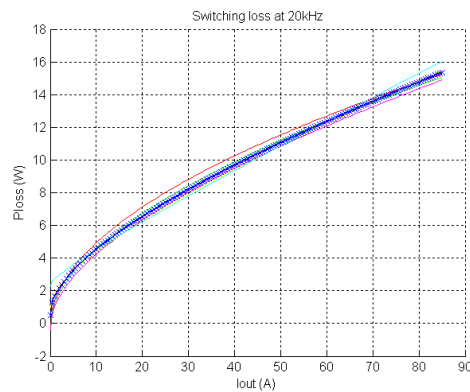


Figure 7 - Switching losses versus output current at 20kHz & Vin = 40V.

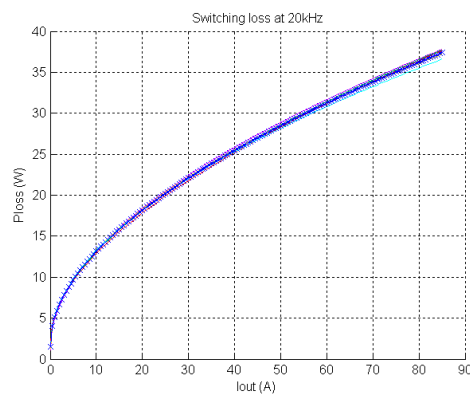


Figure 8 - Switching losses versus output current at 20kHz & Vin = 80V.

5. APPLICATION OF RESULTS

Extracting the coefficients during the fitting allows for ease of integration into any simulation. This is important as it allows the creation of power loss and efficiency contour plots.

Power loss and efficiency contour plots are a good way to display and analyse the performance of a general voltage-current output converter or any variable speed drive.

Figures 9 through 12 show efficiency and power loss contour plots for the 120V system considered throughout this paper. Figures 9 & 10 are without switching loss. Figures 11 & 12 are with the 20kHz switching loss derived in this paper.

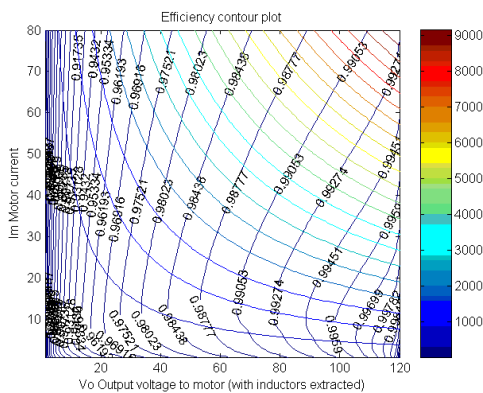


Figure 9 - Non-switching loss efficiency contour plot.

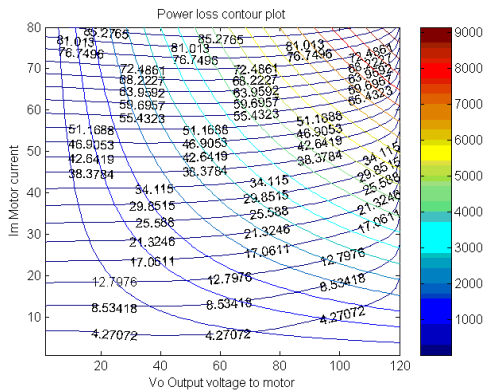


Figure 10 - Non-switching loss power loss contour plot.

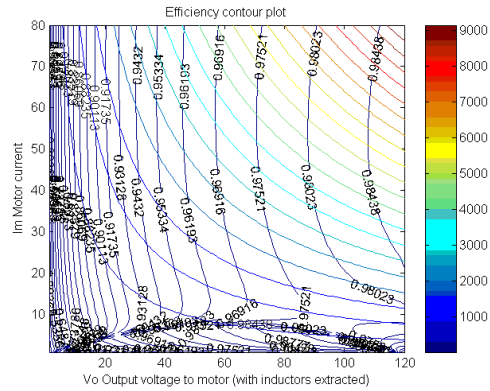


Figure 11 - 120V 20kHz efficiency contour plot.

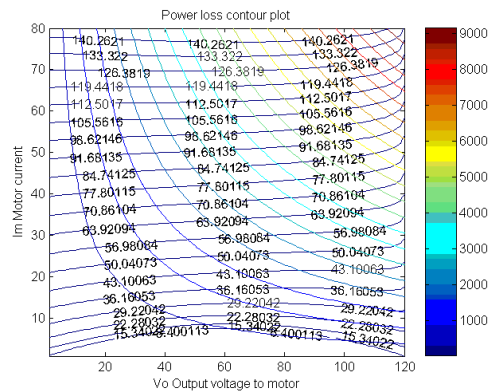


Figure 12 - 120V 20kHz power loss contour plot.

MOSFETs tend to be better in automotive drives due to their power loss being closely related to the square of the output current, hence when compared to IGBTs they have very low loss at the lower currents required for cruising in a car [2]. The square root relation of the reverse recovery charge with the output current tends to negate this effect. This can be seen in Figures 10 & 12, in Figure 10 power loss at 80A is 85W and in Figure 12 it's 140W, a 70% increase. Whereas at 25A (more of a cruising current) Figure 10 is 17W and Figure 12 is 56W, a 330% increase.

6. CONCLUSION

A very simple and quick method for switching loss extraction from a complete converter has been presented in this paper. There is no need for extremely fast oscilloscopes and specialised testing circuits to go with them. There is no need for expensive calorimetric equipment. All that is needed are three multimeters and a current probe.

To verify the measurements, the equivalent resistance, forward drop and constant power draw were found. Given the accuracy of these numbers it appears as if this method could be extended to characterise the complete losses of the converter.

It would be quite simple to automate the system to perform the method presented. This would not only speed up the process but also allow for more data points and hence greater accuracy and extraction of more detailed losses.

As an ultimate verification of the method, a comparison with calorimetric methods is envisaged in the near future.

7. REFERENCES

- [1]. O. Al-Naseem, R. W. Erickson and P. Carlin, "*Prediction of switching loss variations by averaged switch modeling*", IEEE Applied Power Electronics Conference, pp242-8, vol. 1, 2000.
- [2]. D. A. Finn and G. R. Walker, "*A Method of Switch Selection for an Electric Vehicle Drive*", AUPEC, pp287-91, 2001.
- [3]. F. Blaabjerg, J. K. Pedersen and E. Ritchie, "*Calorimetric Measuring System for Characterizing High Frequency Power Losses in Power Electronic Components and Systems*", IEEE Industry Applications Conference, pp1368-76, vol. 2, 2002.
- [4]. D. J. Patterson, "*An Efficiency Optimised Controller for a Brushless DC Machine, And Loss Measurement Using a Simple Calorimetric Technique*", IEEE Power Electronics Specialists Conference, pp22-7, vol. 1, 1995.
- [5]. Ned Mohan, Tore M. Undeland, William P. Robbins, *Power Electronics : converters, applications, and design*, J. Wiley, 1995, p584.
- [6]. Robert W. Erickson and Dragan Maksimovic, *Fundamentals of Power Electronics*, Kluwer Academic Publishers, 2001.
- [7]. IXYS Corp., IXFX120N20 MOSFET data sheet.
- [8]. International Rectifier Corp., IRG4PC30KD IGBT data sheet.
- [9]. Ferroxcube Corp., 3C90 Ferrite material data sheet.
- [10]. Ferroxcube Corp., E65 core data sheet.